THE JOURNAL OF PHYSICAL CHEMISTRY B LETTERS

2005, *109,* 11851−11857
Published on Web 06/02/2005

Boosting Fuel Cell Performance with a Semiconductor Photocatalyst: TiO_2/Pt−Ru Hybrid Catalyst for Methanol Oxidation

Kristine Drew,[†,‡] G. Girishkumar,[†] K. Vinodgopal,[†,§] and Prashant V. Kamat*[,†]

Radiation Laboratory and Department of Chemical and Biomolecular Engineering, University of Notre Dame, Notre Dame, Indiana 46556-0579, and Department of Chemistry, Indiana University Northwest, Gary, Indiana

Received: March 2, 2005; In Final Form: April 15, 2005

A hybrid carbon fiber electrode (CFE) consisting of TiO_2 semiconductor photocatalyst and Pt−Ru catalyst has been developed to boost the performance of direct methanol fuel cells (DMFC). These two catalyst nanoparticles are deposited on opposite sides of the carbon fiber paper such that methanol oxidation is carried out catalytically on Pt−Ru and photocatalytically on TiO_2 under UV-light irradiation. Since both catalysts carry out methanol oxidation independently, we observe an additive effect in the current generation. The carbon support fibers provide a large network to collect the electrons from both of these catalytic processes and thus assist in efficient current generation. In addition, TiO_2 improves the performance of the Pt−Ru catalyst in dark, indicating possible surface area improvement or diminished poisoning effects. The concept of incorporating a photocatalyst provides new ways to minimize precious metal content and enhance the performance of DMFCs. At low catalyst loadings (0.15 mg/cm^2) at 295 K, a 25% enhancement in the peak power density is observed upon illumination with light.

Introduction

For more than two decades, the electrode assembly employed in the operation of a direct methanol fuel cell (DMFC) relies on the Pt−Ru catalyst anchored on a carbon support.[1−4] A proton exchange membrane (PEM) separates the C/Pt−Ru anode and C/Pt cathode and allows ion transport between the two cell compartments. In recent years, efforts have been made to minimize the use of precious metal catalyst by introducing new nanostructured carbon supports and/or less expensive catalysts.[5−7] In a recent study, we demonstrated the use of carbon nanotubes to disperse the Pt catalyst and improve the performance of fuel cells.[8,9] Electrophoretic deposition of carbon nanotubes on electrode surfaces provided an efficient means to disperse platinum catalyst without a binder and decrease the onset potential for methanol oxidation.[9−11]

Large band gap semiconductor materials such as TiO_2 are very effective photocatalysts to carry out oxidation of methanol under UV excitation.[12−18] The charge separation that follows the band gap excitation of semiconductor particles initiates the redox processes at the interface.[19] By suitably casting thin films of TiO_2 particles on an electrode surface, it is possible to collect the electrons and generate current in a photoelectrochemical cell.[20] The principle of photocatalysis has been widely employed in the development of solar cells and environmental remediation processes.[20−33] Under band gap excitation of the TiO_2 electrode, methanol is oxidized by the photogenerated holes, and the photogenerated electrons flow through the external circuit. In addition, Pt deposited on TiO_2 has long been accepted to increase the latter's photocatalytic performance.[18,22,34−42]

SCHEME 1: Catalytic and Photocatalytic Oxidation of Methanol at a Pt/Ru and TiO_2 Modified Carbon Fiber Electrode

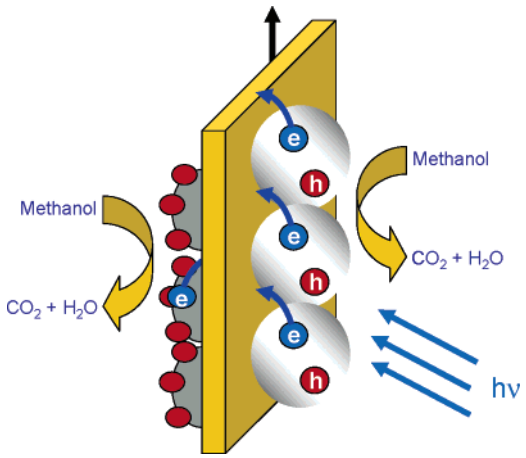

In the past, limited effort has been made to employ oxides such as TiO_2 particles for the design of the cathode and minimize the interference from methanol during oxygen reduction.[43] It was shown that Pt/TiO_2 catalyst exhibits a higher active surface area than Pt and, thus, improves the performance for oxygen reduction.[43,44] Incorporation of transition metal oxides in the anode has been shown to minimize the CO poisoning effects in a methanol fuel cell.[45,46] In the present investigation, we have incorporated TiO_2 particles in the anode along with the Pt−Ru catalyst system to carry out methanol oxidation. We make use of the photocatalytic properties of TiO_2, to boost the traditionally attained current from the oxidation of methanol at the Pt−Ru catalyst system. Scheme 1 illustrates the principle of methanol oxidation at this hybrid electrode. Experiments that demonstrate

* To whom correspondence should be addressed. E-mail: pkamat@nd.edu. Web: http://www.nd.edu/~pkamat.
† University of Notre Dame.
‡ Co-op student from University of Waterloo, Canada.
§ Indiana University Northwest.

10.1021/jp051073d CCC: $30.25

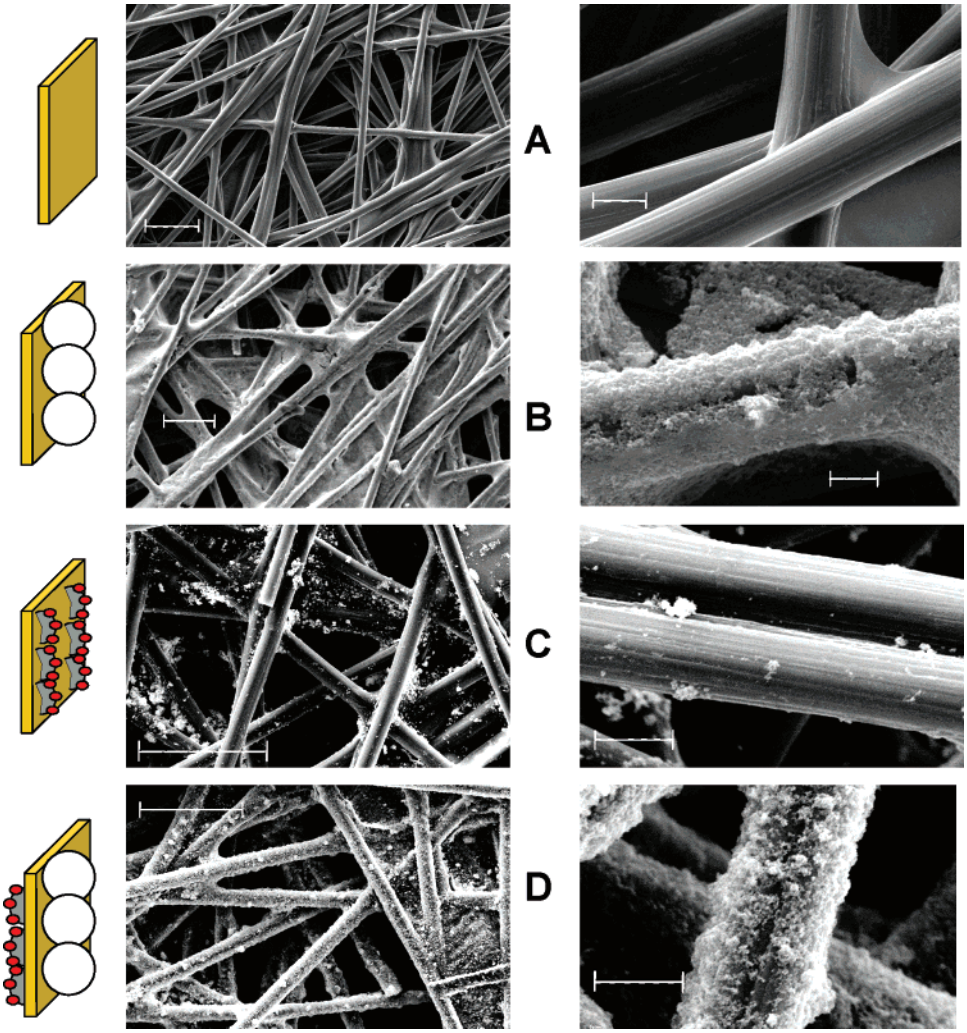

Figure 1. Scanning electron micrograph showing the carbon fiber paper and its modification with TiO_2 and Pt catalyst: (A) CFE, (B) CFE/TiO_2, (C) Pt−Ru/CFE, and (D) TiO_2/CFE/Pt−Ru. (Magnification: Bar in left column represents 50 μm, bar in right column represents 6 μm).

the photocurrent generation via photocatalytic oxidation of methanol at TiO_2 particulates and catalytic oxidation of methanol at Pt−Ru nanoparticles are presented.

Experimental Section

Preparation of TiO_2 and Pt−Ru Electrodes. Cut pieces of Toray paper (Fuelcellstore.com) were used as a carbon fiber electrode (CFE) and further modified with Pt and TiO_2 particles. The carbon fiber network of the paper electrode provides necessary support to anchor catalyst particles and facilitates collection and conduction of electrons. Platinum−ruthenium black catalyst (Pt:Ru nominally 1:1) obtained from Johnson Matthey was suspended in a THF solution containing 1.6% Nafion (diluted from 5% solution obtained from Aldrich). The Pt−Ru catalyst was deposited on the carbon paper by paint brush method and air-dried. Once completely dry, the paper was weighed to determine the catalyst loading. TiO_2 modified CFEs were prepared from a suspension of 5 mg/L TiO_2 (Degussa P-25, mostly anatase) in methanol. The suspension was added dropwise with a microsyringe on the carbon paper electrode, drying with an air stream between microdrops to evaporate the solvent, until the desired amount of TiO_2 was loaded onto the carbon fiber paper. As it has been found that baking the TiO_2 film influences the photoconversion efficiency,[34,47] the TiO_2 modified CFE was then annealed at 473 K for 30 min. These optimum baking conditions were independently determined by recording the photocurrent with CFE/TiO_2 electrodes that were annealed at temperatures in the range of 373−623 K, for periods of time varying from 0 to 4 h.

To construct the hybrid electrodes, the two methods described above for applying Pt−Ru catalyst and TiO_2 were used sequentially, and in that order, on opposite sides of the CFE. These hybrid electrodes serve as anodes for methanol oxidation. For comparative studies, a large sheet of paper was modified with catalysts and then cut into equal pieces so that each electrode to be compared had a uniform catalyst loading over a 1 cm × 1.5 cm area. These electrodes are referred to as CFE/Pt−Ru, CFE/TiO_2, and TiO_2/CFE/Pt−Ru electrodes, respectively. CFE/Pt−Ru electrodes were annealed along with TiO_2/CFE/Pt−Ru electrodes to ensure consistent results.

The anode and cathode (5 cm^2 each) prepared as above were pressed against a Nafion film to build the membrane assembly. This membrane assembly was then inserted into an air breathing methanol fuel cell obtained from Fuelcellstore.com. The side facing the anode was modified with a quartz window to transmit UV light. Polarization curves were recorded by monitoring current and voltage at different load resistances.

Electrochemical and Photoelectrochemical Evaluation of Photocatalyst. Half cell reactions were carried out in a 3-arm electrochemical cell using Pt foil as the counter electrode and a standard calomel electrode (SCE) as the reference electrode. Cyclic voltammetry experiments were carried out using a BAS 100 W electrochemical analyzer. Photocurrent generation and

i−V characteristics of the CFE/TiO_2, TiO_2/CFE/Pt−Ru, and CFE/Pt−Ru electrodes were monitored with and without UV illumination. A 150 W Hg lamp (ORIEL) with a copper sulfate filter (eliminating all wavelengths under 300 nm) was employed as an excitation source, having a measured power density of 28 mW/cm^2 at or near the electrode surface. Photocurrent measurements were conducted using a medium-pressure Hg lamp equipped with quartz optics and monochromator to select the wavelength of excitation, and a Keithley electrometer.

Results and Discussion

Electrode Characterization. The TiO_2 and Pt−Ru catalyst particles cast on carbon fiber paper were analyzed using a Carl Zeiss SMT model EVO 50 XVP scanning electron microscope (SEM). The micrographs taken before and after modification of carbon fiber with TiO_2, Pt−Ru, and TiO_2−Pt−Ru catalysts are shown in Figure 1A−D. Toray paper is made up of layers of fibrous and porous carbon strands. This provides a large surface area and the foundation to disperse the catalysts uniformly. For example, the micrograph in Figure 1B shows that the dispersion of TiO_2 nanoparticles on the carbon fibers is fairly uniform and is bound strongly to the carbon fiber strands. It is interesting to note that the simple drop cast method employed for depositing TiO_2 nanoparticles in the present study provides a high surface area photocatalyst network on CFE.

Although the Pt−Ru and TiO_2 catalysts are applied to opposite sides of the CFE, both solutions disperse throughout the 60 μm thickness fiber network. Appearance of catalyst particles on the opposite side is confirmed visually with the SEM as well as by energy dispersion spectroscopy (EDS used in conjunction with the SEM apparatus, is an INCA Energy 350 produced by Oxford Instruments). The large network of carbon fibers thus assists in maximizing the photoconversion efficiency of TiO_2 photocatalyst by providing a support to disperse catalyst particles, and by assisting in the collection and transport of electrons.

Photoelectrochemical Effect at CFE/TiO_2 Electrodes. TiO_2 is a large band gap semiconductor ($E_g = 3.0$ eV) that undergoes charge separation under UV irradiation. The electrons generated in particulate films can be collected at a conducting electrode surface to generate photocurrent.[20] TiO_2 films cast on optically transparent electrodes have been employed in photochemical solar cells[48,49] and remediation of chemical contaminants in water.[20,50−52] To the best of our knowledge, photoelectrochemical aspects of TiO_2 particles deposited on carbon fiber paper or carbon cloth have not yet been explored fully. It is interesting to probe how the large network of carbon influences the collection of charges and their delivery to the external circuit.

We tested the photoelectrochemical behavior of the TiO_2 photocatalyst by irradiating the CFE/TiO_2 electrode with UV light and recording the photocurrent at different applied potentials. We employed a sacrificial electron donor (methanol) in these experiments to simulate the conditions of DMFC. Upon UV illumination, separation of holes and electrons occurs (reaction 1). Whereas holes are consumed in methanol oxidation, the electrons are collected by the carbon fibers to generate current (reaction 2).

$$TiO_2 + h\nu \rightarrow TiO_2(e + h) \quad (1)$$

$$TiO_2\,(h) + CH_3OH + 6H_2O \rightarrow \rightarrow TiO_2 + CO_2 + 6H^+ + 6e^- \quad (2)$$

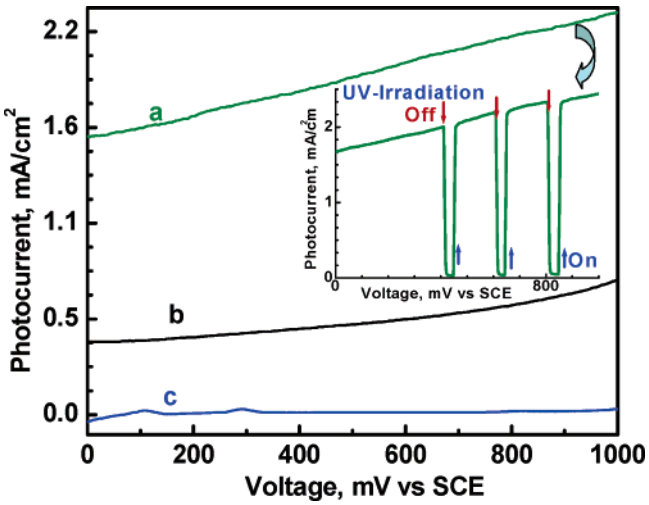

Figure 2. Photocurrent response of CFE/TiO_2 electrodes to UV illumination: (a) annealed CFE/TiO_2 under UV illumination; (b) CFE/TiO_2 with no annealing under UV illumination; (c) annealed CFE/TiO_2 in the dark. The inset shows the photocurrent response of the annealed CFE/TiO_2 electrode when the UV irradiation was turned off and on during the scan of applied potential.

Figure 2 shows the photocurrent response of CFE/TiO_2 electrodes to UV irradiation at different applied potentials. The absence of anodic current in dark (curve c) shows that the methanol oxidation did not occur at CFE/TiO_2 when the UV irradiation was turned off. Comparison of curves a and b in Figure 2 shows that annealing the films at 473K for 30 min produced maximum photocurrent. The inset in Figure 2 shows the photocurrent response to on−off cycles of UV irradiation. The photocurrent generation is prompt and reproducible during the anodic scan. We also varied the TiO_2 loading to maximize the performance of the photoelectrode. With increasing concentration of TiO_2, we harvest more UV photons and observe an increased photocurrent generation. However, at higher loadings, the coverage of TiO_2 is too high to harvest photons and transport electrons efficiently. The optimized photocurrent is seen at a loading of 0.133 mg/cm^2.

The photoresponse of the CFE/TiO_2 electrode was further analyzed by employing monochromatic light for excitation, a technique used in earlier studies.[41,53,54] The fact that the onset of photocurrent is seen at wavelengths below 380 nm confirms that the band gap excitation (>3.0 eV) is necessary to induce charge separation in TiO_2 (Figure 3). At no applied bias, we observe a maximum incident photon to carrier generation efficiency (IPCE) of 14%. At an applied bias of 0.35 V vs SCE, we observe an increase in the maximum efficiency to 34%. This increase in the photoconversion efficiency is attributed to the improved charge separation under the influence of the applied bias which facilitates quick transfer of photogenerated electrons to the external circuit. The photogenerated holes in the electrochemical cell are scavenged by methanol. The methoxy radicals formed during oxidation can further inject electrons and contribute to the increased current generation. This phenomenon is usually referred to as the current-doubling effect and has been discussed in earlier studies.[18,55,56] The photocatalytic oxidation of methanol if adopted in a fuel cell should provide a good additive effect to boost the current generation.

Methanol Oxidation at TiO_2/CFE/ Pt−Ru Electrodes. The electrocatalytic oxidation of methanol at the anode by Pt−Ru is the primary step responsible for the operation of DMFCs. Since TiO_2 anchored on the anode additionally oxidizes

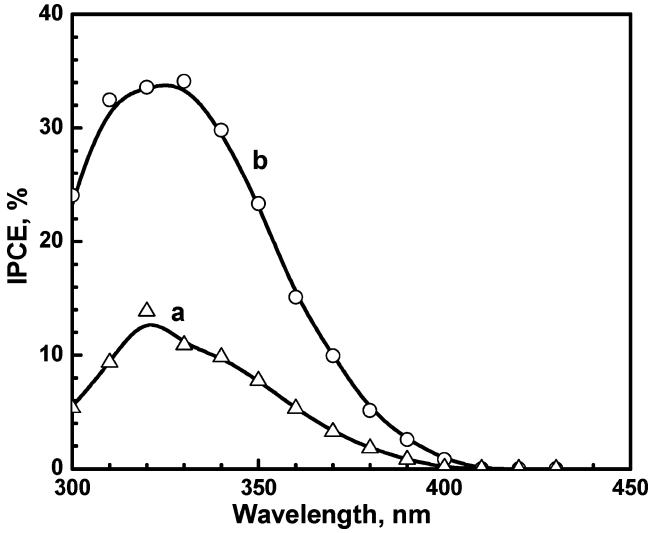

Figure 3. Photocurrent action spectrum of CFE/TiO_2 electrode at (a) no applied bias and (b) at 0.35 V vs SCE. IPCE(%) = 100(1240/λ)-(i_{sc}/I_{inc}) where i_{sc} is short circuit current and I_{inc} is the power of the incident light. Electrolyte was 2.2 M methanol in 1 M H_2SO_4 solution.

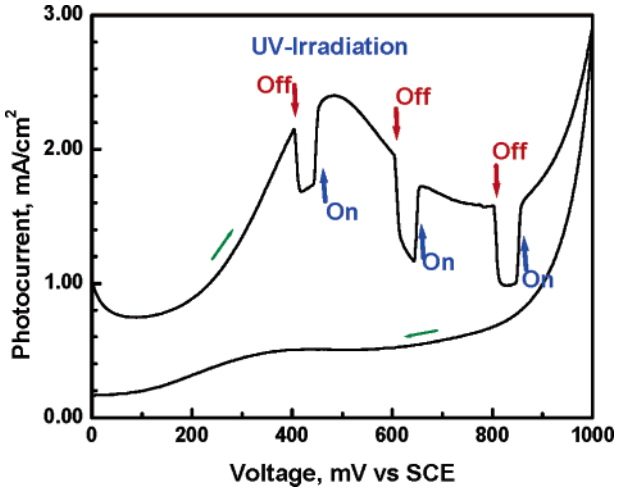

Figure 4. Cyclic voltammogram showing the oxidation of methanol at the TiO_2/CFE/Pt−Ru electrode under UV illumination. The UV irradiation was turned off and on during the scan of applied potential. Electrolyte was 2.2 M methanol in 1 M H_2SO_4 solution.

methanol under UV irradiation, we should be able to enhance the anodic current by coupling the two processes.

$$\text{CFE/Pt−Ru} + \text{methanol} + H_2O \rightarrow \text{CFE(6e)/Pt−Ru} + CO_2 + 6H^+ \quad (3)$$

$$\text{CFE/}TiO_2 + \text{methanol} + H_2O + h\nu \rightarrow \text{CFE/}TiO_2\text{(6e)} + CO_2 + 6H^+ \quad (4)$$

Indeed the cyclic voltammogram of methanol oxidation at TiO_2/CFE/Pt−Ru electrode (Figure 4) shows an increased anodic current when accompanied by UV irradiation. The photocurrent generated at TiO_2 adds to the current arising from the catalytic oxidation at Pt−Ru as emphasized by intermittently turning the light "on" and "off" during the anodic scan (analogous to Figure 2B).

The cyclic voltammogram exhibits a characteristic methanol oxidation peak that one usually observes in a Pt−Ru catalyzed reaction with a peak current around 500 mV vs SCE. The presence of Ru suppresses the poisoning effect caused by CO adsorption on the Pt surface. The electrons collected by the CFE from the two reactions 3 and 4 are delivered to the external circuit, generating enhanced current. This observation supports our argument that the two catalytic processes can function cooperatively, and their respective currents can add to create a greater overall current generation.

Exploring the Synergy of TiO_2 and Pt−Ru Composite Catalyst in Methanol Oxidation. TiO_2/CFE/Pt−Ru electrodes were found to produce significantly higher current than CFE/Pt−Ru electrodes even without light (Pt−Ru loading same on both). The anodic current observed with TiO_2/CFE/Pt−Ru under constant UV illumination is higher than the additive currents observed with CFE/Pt−Ru and photocurrent with TiO_2/CFE electrodes in separate experiments (at constant catalyst loadings). These results indicated an effect apart from photocurrent alone, and the possible synergy of TiO_2 and Pt−Ru catalysts in promoting methanol oxidation.

The enhanced performance of a composite catalyst on methanol oxidation in long-term operation was probed by scanning the electrodes repeatedly. The cyclic voltammograms of CFE/Pt−Ru and TiO_2/CFE/Pt−Ru (Pt−Ru loading of approximately 0.8 mg/cm^2 in both cases) were recorded both in the dark and under UV illumination during multiple scans. Figure 5A compares the cyclic voltammetry curves obtained from the 11th scan.

The cyclic voltammogram characteristics changed slightly as the number of scans progressed. The methanol oxidation peak shifted to higher potential values (about 600 mV), and a peak due to CO poisoning appeared during the reverse scan, indicating the possible poisoning effects during repeated cycling. These characteristics were consistent for all electrodes tested, with or without light or TiO_2.

The maximum current observed for the methanol oxidation increased during initial scans. Figure 5B shows the dependence of maximum current observed for the three cases (TiO_2/CFE/Pt−Ru with and without illumination, and CFE/Pt−Ru without illumination) from the successive cyclic voltammetric scans. For TiO_2/CFE/Pt−Ru electrodes, during the first few scans, we see an increased methanol oxidation current as the catalyst surface gets activated. After attaining a maximum (in this instance after 11 scans), we see a slow decline in the current. This decline is not observed for CFE/Pt−Ru electrodes, for which the peak current density increases slowly and steadily over many scans (although the values are much lower in magnitude than those obtained with TiO_2/CFE/Pt−Ru electrodes). Even after 30 scans, the TiO_2 incorporated Pt−Ru electrodes performed better than the one without TiO_2.

The higher anodic current (trace b compared to trace a in Figure 5B) shows the beneficial role of TiO_2 in improving the catalytic performance of Pt−Ru even in the dark. TiO_2 alone is supposed to be nonactive in the dark. However, its presence near the Pt−Ru catalyst causes the overall performance to improve. Although we deposited the two catalysts on either side of the carbon fiber paper (CFE), there is significant penetration of the catalyst causing some mixing of the catalyst. As discussed in the characterization of the electrodes section, TiO_2 is well distributed and is present on both sides of the TiO_2/CFE/Pt−Ru electrode (Figure 1D), and TiO_2 and Pt−Ru catalysts are in direct contact with each other.

These observations further ascertain that both TiO_2 and Pt−Ru catalysts collectively promote the oxidation of methanol. Although the exact origin of such an enhancement is yet to be determined, three possible reasons come into play: (1) the adsorption of methanol on TiO_2 increases the local concentration

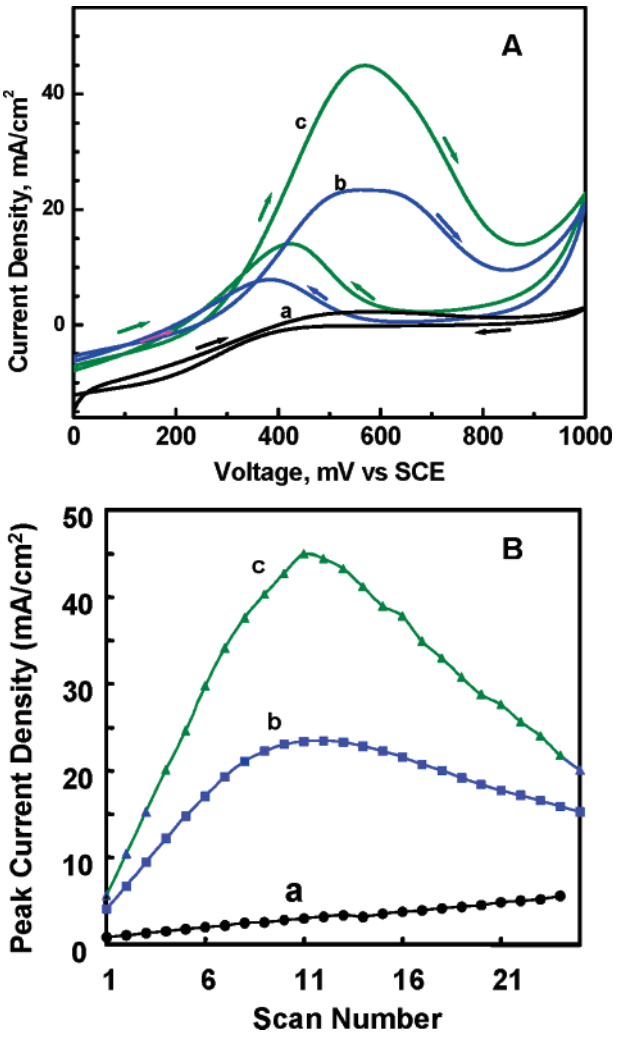

Figure 5. (A) Cyclic voltammograms showing the oxidation of methanol at (a) CFE/Pt−Ru, (b) TiO_2/CFE/Pt−Ru in the absence of light, and (c) TiO_2/CFE/Pt−Ru under UV-illumination. The curves shown here are those obtained on the 11th scan. Electrolyte: 2.2 M methanol in 1 M H_2SO_4. (B) Peak oxidation current density versus the number of repetitive CV scans at (a) CFE/Pt−Ru, (b) TiO_2/CFE/Pt−Ru in the absence of light, and (c) TiO_2/CFE/Pt−Ru under UV illumination.

of methanol around the Pt−Ru catalyst, (2) minimizing the poisoning effects at the anode, and (3) prevention of catalyst aggregation or deformation during the methanol oxidation. Recent studies of developing anodes with transition metal oxides have shown decreased CO poisoning effects in hydrogen fuel cells.[45,46] It has also been reported that TiO_2 supported Pt particles possess a greater electrochemically active surface area for oxygen reduction, decrease the charge-transfer resistance, and decrease the adsorption strength of oxygen and hydrogen compared to bare Pt (no UV illumination was employed in these experiments).[43,44] By using X-ray diffraction, it was demonstrated that Pt and TiO_2 did not complex, but it was suggested that new active sites may be formed at the Pt/TiO_2 interface. Although it has been long accepted that Pt increases TiO_2 photocurrent generation by acting as an electron sink and thus aiding in charge separation,[18,22,34−42] the enhancement caused by the presence of TiO_2 in the Pt catalyzed processes remains to be fully explored. Further analysis of morphological changes of the electrode surface can shed more light into the beneficial aspects of TiO_2 in boosting the performance of Pt−Ru catalyst.

Hybrid Electrode Assembly in the Operation of a Fuel Cell. A fuel cell assembly with a quartz window was employed for evaluating the performance of the TiO_2/CFE/Pt−Ru electrode. Two CFE electrodes (5 cm^2 each) modified with TiO_2 and Pt−Ru (anode) and Pt black (cathode) were pressed on to the opposite side of the Nafion membrane to prepare the PEM assembly and mounted inside the fuel cell. The collector electrode was porous, thus allowing about 40% of the electrode area to UV excitation. The photograph of the air breathing DMFC cell under illumination and the current voltages recorded at different loads under dark and UV irradiation are shown in Figure 6. The Pt−Ru metal loading was 0.15 mg/cm^2, and TiO_2 loading was 0.4 mg/cm^2. The experiments were carried out under static conditions (i.e., without flowing methanol through the anode compartment). The cathode compartment was exposed to air under ambient conditions.

As expected from the photoelectrochemical measurements, the DMFC cell using the TiO_2/CFE/Pt−Ru hybrid electrode responded to UV illumination (Figure 7). The reproducibility of the hybrid electrode response to illumination was confirmed by carrying out repeated on−off cycles of UV illumination. Upon UV illumination of the TiO_2/CFE/Pt−Ru hybrid electrode, an increase in the open circuit voltage (∼200 mV) and short-circuit current of ∼25 mA was seen in the polarization curves of Figure 6. The maximum power delivered by this cell is 3.5 and 4.5 mW in the absence and presence of light. A shift in the power curve toward higher current density is an indication of

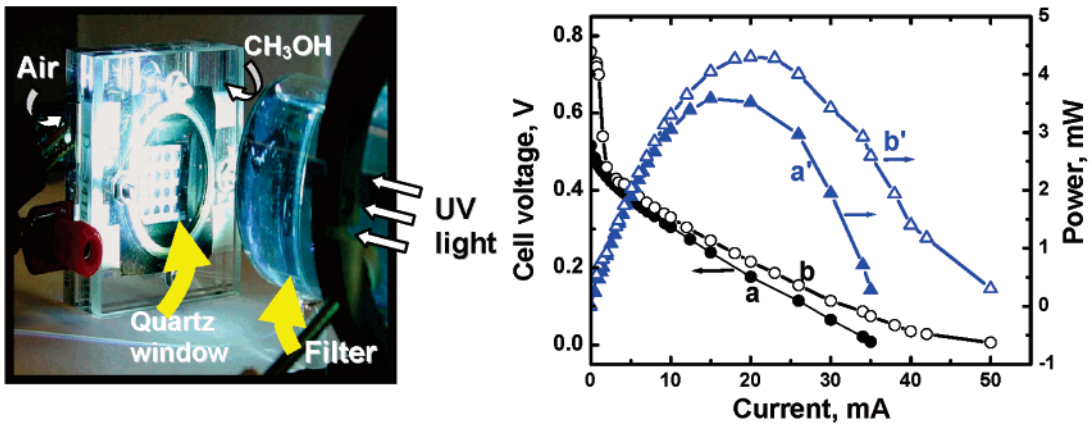

Figure 6. Left. Air breathing DMFC cell equipped with quartz window for UV excitation. Right: Galvanostatic polarization and power output data at 295 K using TiO_2/CFE/Pt−Ru anode and CFE/Pt black cathode Traces were recorded (a) and (a′) in the absence and (b) and (b′) in the presence of UV illumination. The Pt loadings for both cathode and anode were maintained at 0.15 mg/cm^2 and TiO_2 loading of 0.4 mg/cm^2. The electrolyte was aqueous 1 M CH_3OH (electrode surface area 5 cm^2).

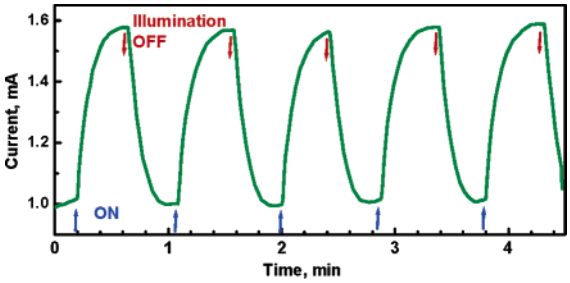

Figure 7. Current response of the cell in Figure 6 to on−off cycles of UV illumination.

the sustainability of the UV-irradiated TiO_2/CFE/Pt−Ru electrode in delivering higher current. These results further ascertain the cooperative effect of TiO_2 and Pt−Ru catalyst in boosting the cell power by ∼25%. It should be noted that the power output of the methanol fuel cell is dependent on the catalyst concentration. The present hybrid cell employs nearly 10 times less catalyst (0.15 mg/cm^2) than those employed in earlier studies (1−2 mg/cm^2).[57−62] Minimizing the catalyst loading is an important issue, and the present study makes an important contribution in this regard.

In addition, the porous metal collector allows only 40% of exposure of the anode. We can expect further enhancement in the power output by employing a mesh type collector electrode that can facilitate irradiation of a larger area of the anode. The technical improvements of the cell design are currently in progress. By means of a simple prototype cell, we have succeeded in demonstrating the use of a photocatalyst for improving the cell performance. Though use of such a photocatalyst is likely to have limited applications, such simple approaches can greatly minimize the use of precious metals yet deliver higher output. In addition, the presence of oxides can also minimize the poisoning effect. Possible applications of such photocatalyst based hybrid cells can be visualized in outdoor fixtures where single stack fuel cells can be spread out to capture sunlight.

Conclusions

Hybrid TiO_2/CFE/Pt−Ru electrodes that catalytically and photocatalytically oxidize methanol have been developed to boost the performance of DMFC. By irradiating the semiconductor hybrid electrode, it is possible to boost the fuel cell power output by ∼30%. This approach is especially attractive as it enables the development of fuel cells with low loadings of Pt−Ru catalyst. The synergetic effects that promote methanol oxidation at Pt−Ru in the dark shows potential application in developing the next generation of fuel cell electrodes.

Acknowledgment. The research described herein was supported by the Indiana 21st Century Research and Technology Fund and the U.S. Army CECOM RDEC through Agreement DAAB07-03-3-K414. Such support does not constitute endorsement by the U.S. Army of the views expressed in this publication. We would like to thank Mr. Ian Duncanson and Mr. James Strope for their assistance in constructing a fuel cell with quartz window for UV illumination. This is contribution NDRL 4583 from the Notre Dame Radiation Laboratory, which is supported by the Office of basic Energy Sciences of the U.S. Department of Energy.

References and Notes

(1) Carrette, L.; Friedrich, K. A.; Stimming, U. *ChemPhysChem* **2000**, *1*, 162.
(2) Wasmus, S.; Kuver, A. *J. Electroanal. Chem.* **1999**, *461*, 14.
(3) Maynard, H. L.; Meyers, J. P. *J. Vacuum Sci. Technol. B* **2002**, *20*, 1287.
(4) Eikerling, M.; Iaselevich, A. S.; Komyshev, A. A. *Fuel Cells* **2004**, *4*, 131.
(5) Cameron, D.; Holliday, R.; Thompson, D. *J. Power Sources* **2003**, *118*, 298.
(6) Kim, W. B.; Voitl, T.; Rodriguez-Rivera, G. J.; Dumesic, J. A. *Science* **2004**, *305*, 1280.
(7) Brune, A.; Jeong, G.; Liddell, P. A.; Sotomura, T.; Moore, T. A.; Moore, A. L.; Gust, D. *Langmuir* **2004**, *20*, 8366.
(8) Vinodgopal, K.; Haria, M.; Meisel, D.; Kamat, P. *Nano Lett.* **2004**, *4*, 415.
(9) Girishkumar, G.; Vinodgopal, K.; Meisel, D.; Kamat, P. V. *J. Phys. Chem. B* **2004**, *108*, 19960.
(10) Kamat, P. V.; Thomas, K. G.; Barazzouk, S.; Girishkumar, G.; Vinodgopal, K.; Meisel, D. *J. Am. Chem. Soc.* **2004**, *126*, 10757.
(11) Nelson, T.; Vinodgopal, K.; Girishkumar, G.; Kamat, P. *One Step Metal Particle Deposition and Solubilization of Single Wall Carbon Nanotubes for fuel cell applications*; Annual meeting of The Electrochemical Society, San Antonio, TX; The Electrochemical Society: Pennington, NJ, 2004.
(12) Peller, J.; Wiest, O.; Kamat, P. V. *J. Phys. Chem. A* **2004**, *108*, 10925.
(13) Micic, O. I.; Zhang, Y.; Cromack, K. R.; Trifunac, A. D.; Thurnauer, M. C. *J. Phys. Chem.* **1993**, *97*, 13284.
(14) Fan, F. R. F.; Liu, H. Y.; Bard, A. J. *J. Phys. Chem.* **1985**, *89*, 4418.
(15) Sobczynski, A. *J. Mol. Catal.* **1987**, *39*, 43.
(16) Oosawa, Y. *Chem. Lett* **1983**, 577.
(17) Ulmann, M.; Augustynski, J. *Chem. Phys. Lett.* **1987**, *141*, 154.
(18) Yamakata, A.; Ishibashi, T.; Onishi, H. *J. Phys. Chem. B* **2002**, *106*, 9122.
(19) Kamat, P. V. *Chem. Rev.* **1993**, *93*, 267.
(20) Vinodgopal, K.; Hotchandani, S.; Kamat, P. V. *J. Phys. Chem.* **1993**, *97*, 9040.
(21) Frank, S. N.; Bard, A. J. *J. Am. Chem. Soc.* **1977**, *99*, 303.
(22) Izumi, I.; Dunn, W. W.; Wilbourn, K. O.; Fan, F. R. F.; Bard, A. J. *J. Phys. Chem.* **1980**, *84*, 3207.
(23) Kamat, P. V.; Karkhanavala, M. D.; Moorthy, P. N. *Sol. Energy* **1978**, *20*, 171.
(24) Decker, F.; Juliao, J. F.; Abramovich, M. *Appl. Phys. Lett.* **1979**, *35*, 397.
(25) Matsumura, M.; Mitsuda, K.; Yoshizawa, N.; Tsubomura, H. *Bull. Chem. Soc. Jpn.* **1981**, *54*, 692.
(26) Nosaka, Y.; Sasaki, H.; Norimatsu, K.; Miyama, H. *Chem. Phys. Lett.* **1984**, *105*, 456.
(27) Knoedler, R.; Sopka, J.; Harbach, F.; Gruenling, H. W. *Sol. Energy Mater. Sol. Cells* **1993**, *30*, 277.
(28) Cao, F.; Oskam, G.; Meyer, G. J.; Searson, P. C. *J. Phys. Chem.* **1996**, *100*, 17021.
(29) Lin, W.-Y.; de Tacconi, N. R.; Smith, R. L.; Rajeshwar, K. *J. Electrochem. Soc.* **1997**, *144*, 497.
(30) Koehorst, R. B. M.; Boschloo, G. K.; Savenije, T. J.; Goossens, A.; Schaafsma, T. J. *J. Phys. Chem. B* **2000**, *104*, 2371.
(31) Tahiri; Serpone, N.; Le van Mao, R. *J. Photochem. Photobiol., A: Chem.* **1996**, *93*, 199.
(32) Horikoshi, S.; Hidaka, H.; Serpone, N. *Environ. Sci. Technol.* **2002**, *36*, 1357.
(33) Bauer, R. *Chemosphere* **1994**, *29*, 1225.
(34) Kraeutler, B.; Bard, A. J. *J. Am. Chem. Soc.* **1978**, *100*, 4317.
(35) Kraeutler, B.; Bard, A. J. *J. Am. Chem. Soc.* **1978**, *100*, 2239.
(36) Ward, M. D.; Bard, A. J. *J. Phys. Chem.* **1982**, *86*, 3599.
(37) Izumi, I.; Fan, F. R. F.; Bard, A. J. *J. Phys. Chem.* **1981**, *85*, 218.
(38) Nosaka, Y.; Norimatsu, K.; Miyama, H. *Chem. Phys. Lett.* **1984**, *106*, 128.
(39) Sadeghi, M.; Liu, W.; Zhang, T. G.; Stavropoulos, P.; Levy, B. *J. Phys. Chem.* **1996**, *100*, 19466.
(40) Wood, A.; Giersig, M.; Mulvaney, P. *J. Phys. Chem. B* **2001**, *105*, 8810.
(41) Subramanian, V.; Wolf, E.; Kamat, P. V. *J. Phys. Chem. B* **2001**, *105*, 11439.
(42) Wang, C. Y.; Pagel, R.; Bahnemann, D. W.; Dohrmann, J. K. *J. Phys. Chem. B* **2004**, *108*, 14082.
(43) Xiong, L.; Manthiram, A. *Electrochim. Acta* **2004**, *49*, 4163.
(44) Shim, J.; Lee, C.-R.; Lee, H.-K.; Lee, J.-S.; Cairns, E. J. *J. Power Sources* **2001**, *102*, 172.
(45) Uribe, F. A.; Valerio, J. A.; Garzon, F. H.; Zawodzinski, T. A. *Electrochem. Solid State Lett.* **2004**, *7*, A376.
(46) Adcock, P. A.; Pacheco, S. V.; Norman, K. M.; Uribe, F. A. *J. Electrochem. Soc.* **2005**, *152*, A459.
(47) Abrahams, J.; Davidson, R. S.; Morrison, C. L. *J. Photochem.* **1985**, *29*, 353.
(48) Graetzel, M. *Nature* **2001**, *414*, 338.

(49) Bisquert, J.; Cahen, D.; Hodes, G.; Rühle, S.; Zaban, A. *J. Phys. Chem. B* **2004**, *108*, 8106.
(50) Vinodgopal, K.; Stafford, U.; Gray, K. A.; Kamat, P. V. *J. Phys. Chem.* **1994**, *98*, 6797.
(51) Stafford, U.; Gray, K. A.; Kamat, P. V. *J. Phys. Chem.* **1994**, *98*, 6343.
(52) Vinodgopal, K.; Bedja, I.; Kamat, P. V. *Chem. Mater.* **1996**, *8*, 2180.
(53) Bedja, I.; Kamat, P. V. *J. Phys. Chem.* **1995**, *99*, 9182.
(54) Boschloo, G. K.; Goossens, A. *J. Phys. Chem.* **1996**, *100*, 19489.
(55) Fujishima, A.; Kato, T.; Maekawa, E.; Honda, K. *Bull. Chem. Soc. Jpn.* **1981**, *54*, 1671.
(56) Harima, Y.; Morrison, S. R. *J. Electroanal. Chem. Interfacial Electrochem.* **1987**, *220*, 173.
(57) Thomas, S. C.; Ren, X. M.; Gottesfeld, S.; Zelenay, P. *Electrochim. Acta* **2002**, *47*, 3741.
(58) Chen, C. Y.; Yang, P. *J. Power Sources* **2003**, *123*, 37.
(59) Choi, W. C.; Woo, S. I. *J. Power Sources* **2003**, *124*, 420.
(60) Dohle, H.; Divisek, J.; Merggel, J.; Oetjen, H. F.; Zingler, C.; Stolten, D. *J. Power Sources* **2002**, *105*, 274.
(61) Larminie, J.; Andrew, D. *Fuel cell systems explained*, 2nd ed.; John Wiley & Sons, Ltd.: New York, 2003.
(62) Piela, P.; Eickes, C.; Brosha, E.; Garzon, F.; Zelenay, P. *J. Electrochem. Soc.* **2004**, *151*, A2053.